

# Interaction Between *n*-octyl- $\beta$ -D-thioglucopyranoside and Bovine Serum Albumin

C. Carnero Ruiz\*, J. M. Hierrezuelo, J. M. Peula-García and J. Aguiar

*Grupo de Fluidos Estructurados y Sistemas Anfífilicos, Departamento de Física Aplicada II, Escuela Universitaria Politécnica, Universidad de Málaga, Campus de El Ejido, 29071 - Málaga, Spain*

**Abstract:** The binding of the nonionic surfactant *n*-octyl- $\beta$ -D-thioglucopyranoside (OTG) to the globular protein bovine serum albumin (BSA) has been investigated by using experimental techniques such as surface tension, steady-state fluorescence and dynamic light scattering. It was observed that the surfactant micellization is delayed in the presence of protein; this was interpreted as a consequence of the fact that part of the surfactant is not available for the formation of micelles, because it is partitioned into the protein hydrophobic sites. This was taken as an evidence of the interaction between surfactant and protein. The fluorescence emission spectra of intrinsic tryptophans revealed that the protein is partially denatured in the presence of high surfactant concentrations. The analysis of the binding features as obtained by two different methods, (i) one based on surface tension measurements, and (ii) another based on the behaviour of the intrinsic BSA fluorescence, indicated that the binding process is non-cooperative at low surfactant concentration, but becomes cooperative when it is high enough. The reduction of the average aggregation number in the presence of protein was interpreted as a sign of the formation of clusters of surfactant adsorbed on the protein surface. A slight conformational change in the protein structure at low surfactant concentration was revealed by resonance energy transfer from tryptophan residues to 8-anilino-1-naphthalene-sulfonate. A treatment of the autocorrelation functions as obtained by dynamic light scattering measurements, based on the application of appropriate fitting techniques, allowed for the discrimination between two kinds of structures in the OTG/BSA system: surfactant-protein complexes, with a "pearl necklace" structure, in equilibrium with the free micelles of OTG.

**Keywords:** Protein-surfactant interactions, binding studies, BSA, OTG.

## INTRODUCTION

The occurrence of interactions between proteins and low molecular weight surfactants has relevance in a number of biotechnological disciplines. The role of these interactions in applications such as drug delivery, cosmetics, or solubilizing processes used for the extraction, isolation and purification of biological macromolecules is decisive. In addition, since the general principles underlying the formation of protein-micellar assembly are common to others like reverse micelles, bilayers, liposomes, and biological membranes [1, 2], a proper understanding on the surfactant-protein interactions is very important because it can be used to our advantage in the choice of the surfactant [3, 4]. Therefore, the characterization of the interactions responsible for the binding of surfactants to proteins has been a subject of extensive study for many years by using a wide range of physical methods [4-6].

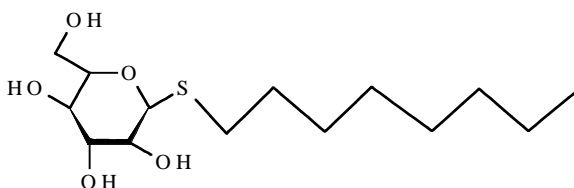
Serum albumins are the most abundant proteins in blood plasma and have the function of incorporating and transporting lipids such as fats, cholesterol and derivatives, into the lymph or bloodstream. Bovine serum albumin (BSA) is a protein that is frequently used for research purposes and as a reference in clinical analyses and biochemistry research due

to its stability, water solubility, and versatile binding capacity [7, 8]. The binding of surfactants to BSA depends on the surfactant nature. For example, it is well-known that anionic surfactants interact strongly with BSA and other proteins causing their denaturation. This effect has been attributed to the ability of these surfactants to associate micelle-like aggregates on the surface of the protein promoting unfolding and, consequently, protein structure alterations [9]. For this reason, many studies have focused on the binding of sodium dodecyl sulfate (SDS) and other anionic surfactants, the studies involving cationic and nonionic surfactants being relatively fewer [8-18].

Because of their favourable physicochemical properties, nonionic surfactants are extensively used in many fields of technology and research [19]. From the point of view of the protein-surfactant interaction the nonionic surfactants are generally less effective than ionic ones, however, there are applications which require to preserve the protein functionality and, hence, the use of nonionic surfactants is preferred. The nature of the interactions responsible for the binding of ethoxylated nonionic surfactants to proteins is being characterized. These investigations indicate that the hydrophobic moiety of surfactants can bind to the non-polar amino acids, whereas the hydrophilic ethyleneoxide chain can interact with the peptide bond and with one or more polar amino acids residues, probably by electrostatic interactions and hydrogen bonding [19, 20]. In many applications in the biomembrane field, which imply solubilization and purifica-

\*Address correspondence to this author at the Grupo de Fluidos Estructurados y Sistemas Anfífilicos, Departamento de Física Aplicada II, Escuela Universitaria Politécnica, Universidad de Málaga, Campus de El Ejido, 29071 - Málaga, Spain; E-mail: ccarnero@uma.es

tion of biopolymers from their natural matrixes by selective solubilization, surfactants with properties such as high solubilizing power, high critical micelle concentration (cmc), no denaturation of proteins, high solubility in water, and stability are required [21]. Alkylpolyglucosides (APGs) are non-ionic surfactants with a hydroxyl sugar group as a hydrophilic moiety, which are attracting increasing interest because they enjoy many of the above properties. Among the APG surfactants, octyl- $\beta$ -D-glucopyranoside (OG) has been probably the most widely used in biomembrane research and reconstitutions processes of biological membranes [22, 23]. Octyl- $\beta$ -D-thioglucopyranoside (OTG) is a related APG surfactant that differs from OG only in how the hydrophilic group is linked by a thioether to the hydrophobic chain (Scheme 1). Its cmc has been determined to be around 8 mM [24], a low value compared to 23 mM [25] for OG, suggesting a more hydrophobic character for the thioglycosylated surfactant. In addition, OTG shows a similar power of solubilization with a higher stability and lower cost [21]. Nevertheless, although OTG has been scarcely used in the biomembrane field, recent investigations [21, 22, 26] showing the advantageous properties of OTG against OG suggest a promising role of the former in that area. Although a few papers dealing with the binding of OTG with polymers have been published [27-30], the interaction between OTG and a globular protein such a BSA seems to have not been studied.



**Scheme 1.** Molecular structure of *n*-octyl- $\beta$ -D-thioglucopyranoside (OTG).

In this paper, we have carried out an experimental study on the interaction between the nonionic OTG surfactant and the protein BSA by using techniques such as tensiometry, steady-state fluorescence, and dynamic light scattering. The present work is intended to be a step toward the characterization of two aspects: the nature of the binding between the protein and surfactant and the structure of the protein-surfactant complexes.

## EXPERIMENTAL

### Materials

All chemicals used were of analytical grade quality. Ultra pure water for the preparation of the solutions (resistivity  $\sim 18 \text{ M}\Omega\cdot\text{cm}$ ) was obtained by passing desionized water through an ultra high quality polishing system (UHQ-PS, ELGA). The surfactant octyl- $\beta$ -D-thioglucopyranoside (OTG) and the protein bovine serum albumin (BSA) used in this work were acquired from Sigma and, due to their high purity grade, were used without further purification. All solutions were prepared in a glycine-HCl buffer of ionic strength 0.1 M in NaCl at pH 5.75. The percentage concentrations of BSA given in this paper are expressed in w/v. The fluorescence probes pyrene and 8-anilinoanthralene-1-sulfonate (ANS) were acquired from Sigma and Fluka, re-

spectively, and were also used as received. The quencher cetylpyridinium chloride (CPyC) was also delivered by Sigma. Stock solutions (1 mM) of the fluorescence probes were prepared in absolute ethanol and stored at 4 °C. From these solutions, work solutions of lower concentration were prepared by dilution. All measurements were carried out with freshly prepared solutions.

### Surface Tension Measurements

The equilibrium surface tension measurements were carried out with a Sigma 701 (KSV) tensiometer by using the Du Nouy ring technique. The system was temperature-controlled at 25 °C by a circulating water bath. The ring was cleaned with distilled water and acetone, and finally flamed. Each series of measurements was started with a concentrated solution of surfactant, and successive diluted solutions were obtained by adding different volumes of buffer or buffered protein solutions to a jacketed vessel. After each dilution, the resultant solution was stabilized for at least 1 h before carrying out the measurement. The surface tension values were accurate within  $\pm 0.1 \text{ mN m}^{-1}$ .

### Fluorescence Measurements

A SPEX FluoroMax-2 steady-state spectrofluorometer was used for the fluorescence experiments. This apparatus is fitted with a 150-W xenon lamp, and equipped with a thermostated cell housing that allowed temperature control to  $\pm 0.1^\circ\text{C}$ . All the fluorescence measurements were made at 25 °C.

The effect of protein on the self-aggregation of OTG was followed by the pyrene 1:3 ratio method [31]. Fluorescence emission spectra of OTG solutions containing around 1  $\mu\text{M}$  pyrene were recorded between 360 and 500 nm by using an excitation wavelength of 335 nm. From these spectra the intensities  $I_1$  and  $I_3$  were measured at the wavelengths corresponding to the first and third vibronic band located near 373 and 384 nm. The ratio  $I_1/I_3$  is the so-called pyrene 1:3 ratio index.

In order to examine the effect of the surfactant addition on the intrinsic fluorescence of BSA, fluorescence emission spectra of solutions containing a fixed protein concentration (30  $\mu\text{M}$ ) and different surfactant concentrations were recorded by using an excitation wavelength of 295 nm and bandwidth of 2.0 nm.

The determination of the mean aggregation numbers ( $N_{agg}$ ) was performed by the steady-state fluorescence quenching method [32]. In all the quenching experiments pyrene was used as a luminescence probe and CPyC as a quencher. Stock solutions containing pyrene (3  $\mu\text{M}$ ), and surfactant (90 mM), were prepared in either buffer solution or protein solutions of different concentrations. Working solutions of lower concentration (1  $\mu\text{M}$  in pyrene and 30 mM in surfactant) were prepared by adding appropriate volumes of quencher solutions. In these studies, the quencher concentrations employed were maintained low enough ( $< 0.18 \text{ mM}$ ) so as not to interfere with the assembly of the surfactant. From these solutions, fluorescence intensities were recorded by using excitation and emission wavelengths of 335 nm and 383 nm, respectively. Triplicate experiments were carried out for each system with different protein content. The errors

**Table 1.** Parameters Obtained from the Data Treatment Based on the Surface Tension Measurements for the BSA/OTG System at 25 °C

BSA (% w/v)	cmc or (cac) <sub>app</sub> <sup>(a)</sup> (mM)	$a \cdot 10^3$ (mmol/m <sup>2</sup> )	$\Gamma_p^0 \cdot f \cdot 10^3$ (mmol/m <sup>2</sup> )	$K_s \times 10^{-3}$ (L/mol)	$(C_s)_{\text{sat}}$ (mM)	$(C_s^f)_{\text{sat}}$ (mM)	$\nu_{\text{sat}}$
0	7.2 (7.1)	3.74	---	---	---	---	---
0.1	8.5 (9.8)	4.08	2.58	8.69	8.4	7.2	78.7
1	10.1 (12.1)	4.45	2.68	5.98	10.1	7.2	19.3

<sup>(a)</sup>Within parenthesis are the cmc or (cac)<sub>app</sub> values as obtained by the pyrene 1:3 ratio method.

in  $N_{\text{agg}}$ , in terms of the standard deviation of three individual determinations, are estimated to be less than 3%.

Resonance energy transfer experiments from tryptophan (Trp) residues of BSA (donor) to ANS (acceptor) were carried out. In these experiments, solutions containing a fixed protein concentration (30  $\mu\text{M}$ ), different surfactant concentrations (2 and 20 mM), and increasing concentration of acceptor were employed. Fluorescence emission spectra of these solutions were recorded under the same optical conditions than in the BSA intrinsic fluorescence assays. From these spectra, fluorescence intensities corresponding to the peaks of the donor (~340 nm) and acceptor (~460 nm) were measured.

### Dynamic Light Scattering Measurements

All dynamic light scattering (DLS) measurements were made in a Zetasizer Nano-S instrument (Malvern Instrument, UK). This apparatus uses the backscattering detection (scattering angle  $\alpha = 173^\circ$ ) and is equipped with an avalanche photodiode detector (APD), a Helium-Neon laser source (wavelength 633 nm; power 4.0 mW), and a thermostated sample chamber controlled by a thermoelectric Peltier. In these studies we use solutions with a fixed protein concentration (30  $\mu\text{M}$ ) and increasing surfactant concentrations, ranging from the pre-micellar to post-micellar region. In addition, we also examine single system constituted by only either BSA (30  $\mu\text{M}$ ) or OTG employing a concentration well above of the critical micelle concentration (20 mM). All these measurements were made at  $25.0 \pm 0.1^\circ\text{C}$ .

## RESULTS AND DISCUSSION

### Interaction of OTG with BSA

In order to obtain information on the interaction of OTG to the protein we have firstly followed the aggregation of the surfactant in the presence of BSA by using the well-documented pyrene 1:3 ratio method [31]. In these experiments, the pyrene 1:3 ratio index was obtained as a function of the surfactant concentration at a fixed protein concentration. The results that we have obtained are shown in Fig. (1). In this figure, it can be seen that in all the cases the plots show a characteristic sigmoidal decrease as the surfactant concentration increases, indicating the transition between the pre- to post-micellar region. There is a remarkable difference between the plots in the absence of protein to those in its presence. Note that in the presence of BSA, and in the pre-micellar region, the pyrene 1:3 ratio values are considerably lower than those corresponding to the pure surfactant, suggesting that the probe is solubilized in the hydrophobic sites

of the protein. However, as soon as the micelles of surfactant are formed the probe is preferentially solubilized in the micellar environment. A similar behaviour has been previously observed in other protein-nonionic surfactant systems [33, 34]. From data in Fig. (1) in the absence of protein, the cmc value of the surfactant was obtained by using the data treatment previously described [35]. Briefly, the experimental data were fitted to a Boltzmann sigmoid type curve, the centre of the sigmoid being identified as the cmc value. It is to be noted that the cmc value obtained compares well with those previously reported for OTG in 0.1 M NaCl [36]. The free surfactant concentration at which aggregation starts to occur in the presence of a polymer is often referred to as the critical aggregation concentration. However, as data in Fig. (1) are plotted in terms of total surfactant concentration, the point at which the transition occurs is an apparent critical surfactant concentration, (cac)<sub>app</sub>. The (cac)<sub>app</sub> values were also determined by using the previous data treatment (see Table 1). Data in Fig. (1) and Table 1 show that, in the presence of BSA, the transition is shifted to higher concentrations of OTG. This fact indicates that part of the surfactant is no longer available for forming micelles. That is, the shift to the right of the curves in Fig. (1) reveals partitioning of the surfactant into new sites, probably the hydrophobic patches of the protein. This partitioning indeed reveals interaction of the surfactant with these hydrophobic sites.

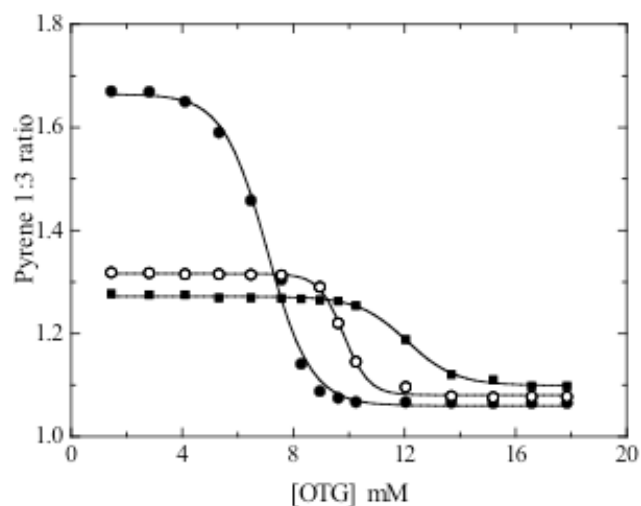


**Fig. (1).** Plot of pyrene 1:3 ratio vs. the total concentration of OTG at different BSA concentrations: (●) 0, (○) 0.1 %, (■) 1.0 %.

In addition, we have also followed the effect of the protein addition on the OTG aggregation by using surface ten-

sion measurements. Fig. (2) shows the results of these experiments. From this figure, it can be observed that, although the tensiometric plots in the presence of BSA follow a similar trend to that of the pure surfactant, the curves are shifted to higher OTG concentrations. This behaviour agrees with that observed in Fig. (1), and indicates interaction of the surfactant with the available sites of the protein, as discussed above. It is observed in Fig. (2) that each plot exhibits a sharp break showing the transition from the pre- to post-micellar region. According to the above reasoning, these break points can be assigned either to the cmc or  $(cac)_{app}$ , in the absence or presence of protein, respectively. In Table 1 we have listed the values corresponding to the break points of the plots in Fig. (2). Except in the absence of protein, the values obtained by the pyrene 1:3 ratio method are higher than those obtained by surface tension measurements, in accordance with usual results obtained by using probe-based measurements [34].

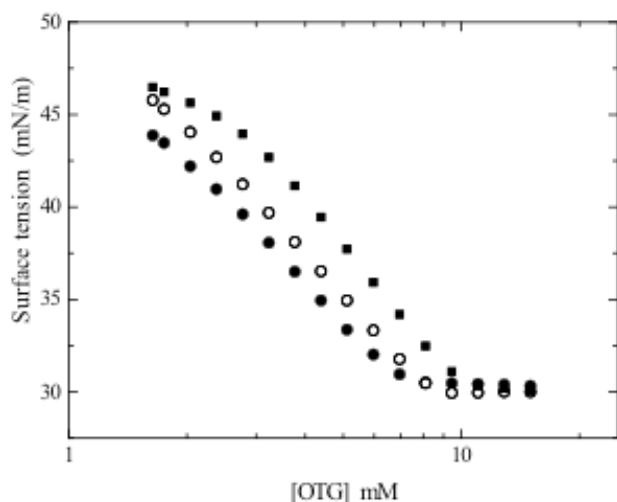


**Fig. (2).** Surface tension of OTG solutions vs. the total surfactant concentration at 298 K in varying BSA concentrations: (●) 0, (○) 0.1 %, (■) 1.0 %.

Another relevant aspect in Fig. (2) is that, above the break point, all plots show surface tension constant values, which are practically independent of the protein concentration. This fact suggests that in the post-micellar region the pure surfactant seems to control the surface tension in the air-liquid interface and, hence, it can be assumed that BSA/OTG complexes are surface inactive species. It is to be noted that a similar behaviour to that shown in Fig. (2) has been previously reported by several authors for different protein-nonionic surfactant systems [34, 37-40].

### Fluorescence of BSA

From a spectroscopic point of view, BSA is mainly characterized by the presence of two tryptophan (Trp) residues ( $W^{135}$  and  $W^{214}$ ), which contribute greatly to the intrinsic fluorescence of BSA. It has been proposed that the Trp residue located at position 135 ( $W^{135}$ ) is buried in a hydrophobic pocket and lies near the surface of the albumin molecule in the second helix of the first domain, whereas that located at position 214 resides in the hydrophobic cavity of the IIA subdomain, corresponding to the so-called Sudlow I binding region [11, 12]. Interaction of BSA with surfactants is usu-

ally accompanied by changes in fluorescence intensity and shifts in the emission maximum, which are mainly attributed to changes in the position or orientation of the Trp residues, altering their exposure to solvent and producing modifications on the quantum yield. Therefore, fluorescence studies can be used to monitor changes on the tertiary structure of the protein induced by the surfactant binding [11]. Changes in the Trp microenvironment upon binding of surfactants can be identified by following emission band occurring in the range of 320–360 nm [8, 9, 11, 12]. Fig. (3) shows representative fluorescence spectra of BSA, at different surfactant concentrations. In this figure, it is observed that with OTG concentration increasing, the fluorescence is quenched and the maximum emission wavelength is blue shifted. It is interesting to remark that the behaviour shown in Fig. (3) is similar than that observed by Tabak and co-workers with different ionic surfactants [11, 12], but is more pronounced than that recently observed in the case of Triton X-100 [20]. In the absence of surfactant, it can be seen a band centred at 345 nm, which is clearly associated to native BSA. At low surfactant concentration ( $2 \text{ mM} < \text{cmc}$ ), it is seen that OTG produces a decrease of the Trp fluorescence and slight blue shift of the emission maximum (343 nm). This spectrum corresponds to a BSA/OTG complex, indicating interaction between surfactant and protein, but where protein denaturation does not occur. The third spectrum, at high surfactant concentration ( $20 \text{ mM} \gg \text{cmc}$ ), presents an emission maximum at 331 nm, indicating the presence of partially denatured species [11, 12].

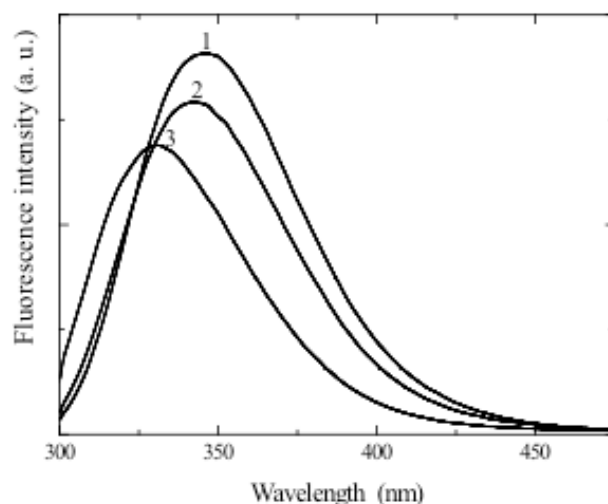


**Fig. (3).** Fluorescence spectra of BSA ( $30 \mu\text{M}$ ) in: (1) the absence of surfactant, (2) the presence of 2 mM OTG, and (3) the presence of 20 mM OTG.

### Binding of OTG to BSA

The nature of the interactions between proteins and surfactants can be better understood by analyzing the binding process of the surfactant on the protein or binding isotherm [41]. We have carried out binding studies by using two different procedures. First of all, binding was quantified by application of the method proposed by Nishikido *et al.* [37], which is based on surface tension measurements. This method has been previously applied to different hydrophilic protein-nonionic surfactant systems, including  $C_{12}E_6$ /BSA

and C<sub>12</sub>E<sub>6</sub>/lysozyme [37], and Triton X-100/BSA [38]. Afterwards, Nishiyama and Maeda [39] applied a simplified version of that approach to examine the binding between a number of ethoxylated nonionic surfactants and lysozyme.

The method proposed by Nishikido *et al.* [37] relies on the assumption that the protein-surfactant complexes are surface inactive. This assumption is supported by the experimental observation that the surface tensions in the post-micellar region are, within the experimental error, identical (see Fig. 2), and it has been attributed to the fact that the hydrophobic areas of protein and surfactant are almost hidden by the formation of the complex [37]. The aforementioned authors proposed an expression for the surface tension of the air-liquid interface of the surfactant in the presence of protein,  $\gamma$ , given by

$$\gamma = -a RT \ln \left[ a + K_s \left( a - \Gamma_p^0 f \right) C_s^f \right] + \gamma_p + a RT \ln a \quad (1)$$

where  $a$  refers to the maximum adsorption of surfactant,  $K_s$  the Langmuir constant for adsorption of the surfactant at the air-liquid interface,  $\Gamma_p^0$  and  $\gamma_p$  are the amount of adsorbed protein at the air-liquid interface and the surface tension of solutions containing the same concentration of protein but no surfactant,  $f$  is the ratio between maximum surfactant adsorption and maximum protein adsorption, and  $C_s^f$  is the concentration of surfactant monomer or the free surfactant concentration. In the case of a pure surfactant solution, the surface tension is given by

$$\gamma_s = -a RT \ln \left[ 1 + K_s C_s^0 \right] + \gamma_{\text{water}} \quad (2)$$

where  $C_s^0$  is the concentration of pure surfactant, and  $\gamma_{\text{water}}$  is the surface tension of pure water. If one assumes that, at the surfactant concentration at which the surface tension becomes constant, the surfactant monomers start forming micelles, and that the monomer concentration is equal to the cmc of the surfactant alone, and since the surface tension above the break point is roughly constant, as previously stated (see Fig. 2), from equations (1) and (2) the following equations can be obtained.

$$\gamma_{\text{cmc}} = -a RT \ln \left[ 1 + K_s \text{cmc} \right] + \gamma_{\text{water}} \quad (3)$$

$$\Gamma_p^0 f = \frac{a(1 + K_s \text{cmc}) \left\{ 1 - \exp \left( -\frac{\gamma_{\text{water}} - \gamma_p}{a RT} \right) \right\}}{K_s \text{cmc}} \quad (4)$$

In this way, by introducing the surface tension data in equations (1), (3), and (4) the average number of bound surfactant monomers per protein molecule,  $\nu$ , can be obtained through the equation

$$\nu = \frac{C_s - C_s^f}{C_p} \quad (5)$$

being  $C_s$  the total surfactant concentration. The treatment followed to obtain the different parameters and the corresponding  $\nu$  value has been previously described [37]. Fig. (4)

shows a representative plot of the free surfactant concentration as a function of the total surfactant concentration in the presence of 0.1 % BSA, as determined by using the mentioned treatment to the experimental data in Fig. (2). Data in Fig. (4) show that the concentration of free surfactant,  $C_s^f$ , increases linearly with the total surfactant concentration until reaching a saturation value,  $(C_s^f)_{\text{sat}}$ , which allows for the

determination of the saturation average number of bound surfactant monomers per protein molecule,  $\nu_{\text{sat}}$ . All data that we have obtained by using this treatment are summarized in Table 1. From data in Table 1 it is observed that the  $\nu_{\text{sat}}$  value becomes smaller as the protein concentration increases, in agreement with the results of Nishikido *et al.* for the C<sub>12</sub>E<sub>6</sub>/BSA system [37]. This fact can be rationalized as follows. It is generally assumed that nonionic surfactants bind to hydrophobic regions of proteins through hydrophobic interactions. It is expected that the number of these hydrophobic regions, which are surfactant-binding sites, decreases as a consequence of the protein-protein interactions within the protein aggregates; this effect being enhanced by the increase in protein concentration [37]. Therefore, the low  $\nu_{\text{sat}}$  value in the presence of 1 % BSA can be attributed to the major probability of formation of BSA aggregates at high protein concentration. In addition, when judging the results obtained from the present method it is important to take into account that the model assumes that, at the surfactant concentration where the surface tension begins to stay constant, surfactant monomers begin to form micelles and the concentration of monomers remains identical with the cmc of the surfactant alone, as shown in Fig. (4). At this point, the saturation occurs and, hence, the added surfactant is employed in forming free micelles but is not adsorbed on the protein. Therefore, it is more than probable that the saturation values of  $\nu$  reported by the present procedure are underestimated. Anyway, it is to be noted that the  $\nu_{\text{sat}}$  values obtained for OTG are considerably higher than those obtained for other conventional ethoxylated nonionic surfactants [37, 38].

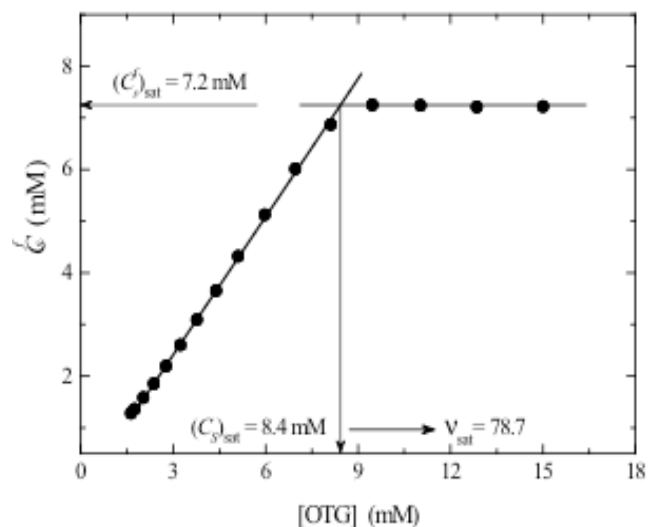


Fig. (4). Free surfactant concentration,  $C_s^f$ , versus the total surfactant concentration in the presence of 0.1 % BSA.

Alternatively, additional information on the binding process between surfactant and protein can be obtained by evaluating the fraction of protein occupied by surfactant [13, 41]. With this purpose, we have followed the change in the intrinsic fluorescence of BSA on addition of OTG. The procedure consists in monitoring the fluorescence of the Trp residues by using solutions with a fixed protein concentration (30  $\mu$ M) and increasing surfactant concentrations. In this way, the fractional change of protein fluorescence due to surfactant binding,  $\theta$ , was calculated by [13, 41-44]

$$\theta = \frac{I_{\text{obs}} - I_f}{I_{\text{min}} - I_f} \quad (6)$$

where  $I_{\text{obs}}$  is the fluorescence intensity at any surfactant concentration,  $I_f$  is the fluorescence intensity in the absence of surfactant and  $I_{\text{min}}$  is the fluorescence intensity under saturation binding condition. It must be noted that this procedure does not measure the average number of surfactant molecules per protein molecule,  $\nu$ , but the fractional occupation of surfactant binding sites [41]. That is, if a BSA molecule has  $n_0$  available binding sites for a determined surfactant and at a certain stage surfactant molecules bind to  $n$  sites, then the fraction of BSA occupied by surfactant is  $\theta = n/n_0$  [13]. In other words, in the presence of surfactant  $I_{\text{obs}} = I_f$  and  $\theta = 0$ , and when the saturation is reached and all the possible sites of BSA are occupied by the surfactant  $I_{\text{obs}} = I_{\text{min}}$  and, hence,  $\theta = 1$ . In this regards, it is important to remark that some authors have used the following formula to determine the average number of surfactant molecules bound per protein molecule,  $\nu$ , [42-44]

$$\nu = \theta \frac{[S]}{[P]} \quad (7)$$

where  $[S]$  and  $[P]$  are the total surfactant and protein concentration, respectively. By using equation (7) one assumes that the term  $(\theta [S])$  yields the concentration of bound surfactant, but it is evident that this assumption is not correct.

The change of the intrinsic fluorescence intensity of BSA,  $I_{\text{obs}}$ , upon surfactant addition is plotted in Fig. (5). It can be observed that binding of surfactant is initially accompanied by quenching of  $I_{\text{obs}}$ , but starting from a certain surfactant concentration the fluorescence intensity remains roughly constant ( $I_{\text{min}}$ ). The inset in Fig. (5) shows the binding curve as obtained by plotting the fractional occupation of protein,  $\theta$ , against the total surfactant concentration. In order to interpret this binding curve is convenient to remember the general characteristics of a binding isotherm between a surfactant and a protein. A binding isotherm shows the average number of surfactant molecules bound per protein molecules,  $\nu$ , as a function of the logarithm of the free surfactant concentration. Following to Jones [45], the binding isotherm of an ionic surfactant to a protein consist of four characteristic regions. In the first region, at lowest surfactant concentration, there are some binding to specific high-energy sites of the protein. This region is followed by either a plateau or a slow rising part, where a binding of non-cooperative character occurs. The third region is characterized by a massive increase in binding due to cooperative interactions. Lastly, the binding curve reaches a plateau indicating the saturation

in the binding process. Although our binding curve (inset in Fig. 5) does not admit a direct comparison with the Jones's model, we can extract some conclusions about how the binding sites of the protein are occupied by the surfactant. First of all, at low surfactant concentration it is observed (see inset in Fig. 5) a slight increase of the fractional occupation,  $\theta$ , with the surfactant concentration. However, from a certain surfactant concentration ( $\approx 1$  mM),  $\theta$  increases steadily until reaching the saturation value. This behaviour seems to reflect an initial non-cooperative binding process at low surfactant concentration, where the hydrophobic interactions play probably a predominant role, which becomes cooperative when the surfactant concentration is high enough. The plateau corresponds clearly to the saturation binding region.

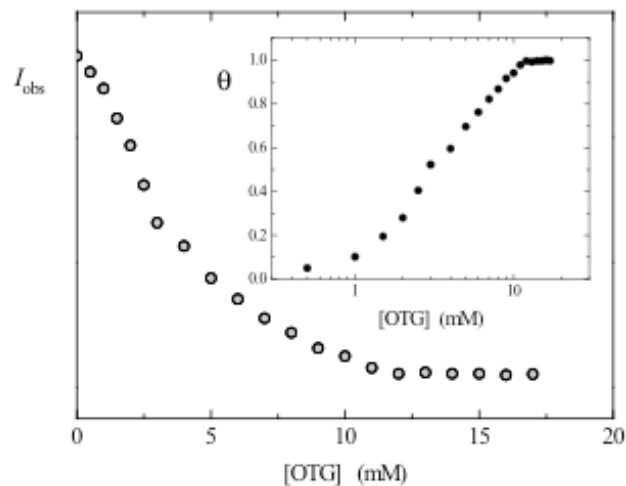


**Fig. (5).** Intrinsic fluorescence of BSA (30  $\mu$ M) as a function of the total surfactant concentration. Inset: Binding curve, showing the fraction of a protein molecule bound by surfactant ( $\theta$ ) as a function log of the total surfactant concentration, for the interaction between BSA and OTG.

With regards to the nature of the interactions involved in the binding process, it is important to mention that previous studies on interactions between nonionic surfactants and BSA indicate that the binding takes place through the condensation of nonionic surfactants onto non-polar areas of the protein surface [5]. This conclusion agrees well with different experimental observations showing that the binding of nonionic surfactants is associated with rather small enthalpy changes comparable with those involved in the micellar formation [46, 47]. Nielsen *et al.* [48] have studied, by using high sensitivity isothermal titration calorimetry, the interaction between BSA and a number of surfactants with C12 acyl chains, including two nonionic surfactants such as hepta- and penta(ethylene glycol) monododecyl ether ( $C_{12}E_7$  and  $C_{12}E_5$ ). These authors found that, in the case of the nonionic surfactants, the binding enthalpy is considerably larger than for any of the anionic surfactants, suggesting that some electrostatic interactions are considered to contribute favourably to the binding enthalpy. In order to explain these observations, the aforementioned authors proposed a possible mechanism based on the existence of hydrogen bonding between the ethylene glycol chain and the protein. However, they could not conciliate this contribution with a large positive heat capacity change associated with the binding process. Like-

wise, Singh and Kishore [20] have recently found that the polar interactions play an important role in the binding between Triton X-100 and BSA.

In relation to the possible contribution of the electrostatic interactions in the case of OTG, it is important to mention that, according to previous studies, the hydrophilic group of OTG behaves more similarly to that of certain homologous series of ionic surfactants, including alkyl sulphates and alkyltrimethylammonium bromides, than to the nonionic ones [24]. In fact, the existence of a small but significant charge in micelles formed by APG surfactants has been previously established [49]. According to this view, a relatively larger contribution of the electrostatic interactions in the case of OTG, as compared with the other conventional nonionic ethoxylated surfactants, should be expected. This could serve as an explanation of the high observed affinity of OTG on BSA, as well as of the fact that this surfactant causes some denaturation in the protein, as deduced from the observed alterations in the intrinsic fluorescence of BSA. In addition, the binding behaviour of OTG may, at least in part, be explained by two aspects: the high cmc value of OTG, which will delay the competition between the binding process and the micellar formation, and the high capacity of APG surfactants to form hydrogen bonds between the hydroxyl groups of their head-groups and the protein.

### Average Aggregation Numbers

If the binding process between OTG and BSA is dominated by a cooperative mechanism accompanied by a partial denaturation of the protein, as suggested by our above findings, the formation of clusters of surfactants adsorbed onto the protein surface is expected. In order to corroborate this expectation we have carried out the determination of aggregation numbers of OTG in the absence and in the presence of protein. With this purpose, we have used the well-established static quenching method [32]. The applicability of this method in protein-surfactant systems has been widely discussed by Vasilescu *et al.* [33]. These authors focused the discussion in the problem of determining the solubilization site of probe and quencher, since these species can be localized in different environments, including the free micelles, the micelle-like aggregates adsorbed on the protein, and the specific sites of the protein. Because it is impossible to differentiate between these situations, they determined the aggregation numbers as if all surfactant, probe, and quencher were micellized. Taking into account this assumption, they obtained similar results by the application of both static and dynamic quenching methods.

We have performed our experiments of fluorescence static quenching by using pyrene as a probe and CPyC as a quencher, as this pair ensures the fulfilment of the appropriate requirements for the application of this method [50]. The results of the quenching experiments were analyzed by using the equation

$$\ln \frac{I_0}{I} = \frac{N_{agg}}{[S] - cmc} [Q] \quad (8)$$

where  $I_0$  and  $I$  are the fluorescence intensities in the absence and presence of quencher, respectively,  $N_{agg}$  is the mean aggregation number,  $[S]$  is the total surfactant concentration,

and  $[Q]$  is the quencher concentration. The fluorescence intensities at 383 nm were plotted according to equation (8) (plots not shown), and an acceptable linear relationship ( $r > 0.99$ ) was observed in all the cases. From these plots, we have obtained the  $N_{agg}$  values in aqueous medium and in the presence of 1% BSA. The mean aggregation number that we have obtained in the absence of protein was  $107 \pm 1$ , a lower value than that previously reported by using static light scattering measurements (114 in pure water and 144 in 0.1 M NaCl) [36]. In the presence of 1% BSA we have found that the aggregation number value is considerably reduced ( $44 \pm 1$ ). A similar behaviour was observed by Vasilescu *et al.* [33] in a number of protein-surfactant systems, including those constituted by the nonionic surfactant  $C_{12}E_8$  and the proteins BSA and lysozyme, and by us in the case of the MEGA-10/BSA system [34]. A reduction of the aggregation number in polymer-surfactant systems has been previously reported, and this change has been considered as a strong evidence of interaction between polymer and surfactant [51]. In our case, the aggregation number obtained in the presence of protein is probably the average value of two types of aggregates: the free micelles and the micelle-like aggregates adsorbed on the surface protein by hydrophobic interactions. In other words, this result is consistent with the formation of a necklace structure for the protein-surfactant complexes [14], where the micellar clusters, smaller than the free micelles, should be adsorbed on the protein surface.

### Resonance Energy Transfer Studies

It has been previously established that the binding mechanism between surfactant and protein is often accompanied by some conformational change in the protein structure as a result of the interactions involved in the process [33]. In order to analyze this aspect we have carried out studies of resonance energy transfer (RET) from Trp residues of BSA to ANS as an exogenous acceptor. RET processes have been widely used to obtain structural and dynamic information on several macromolecular assemblies, including macromolecule-ligand complexes, polymer-surfactant and protein-surfactant systems [42, 52, 53].

According to the Foster's theory, the rate constant for RET,  $k_{ET}$ , occurring by dipolar interactions between a donor and an acceptor is given by [54]

$$k_{ET} = \frac{8.8 \cdot 10^{-25} K^2 \Phi_D J}{n^4 \tau_D R^6} \quad (9)$$

where  $K^2$  is a factor describing the relative orientation in space of the transition dipoles of donor and acceptor,  $n$  is the refractive index of the medium,  $\tau_D$  and  $\Phi_D$  are the lifetime and the quantum yield for the donor in the absence of the acceptor, and  $J$  is the spectral overlap integral between donor emission and acceptor absorption. From equation (9) it is evident the strong dependence of RET process on the distance  $R$ , hence, RET studies are especially useful to estimate changes in the separation distance between donor and acceptor. It is also observed from equation (9) that  $k_{ET}$  depends directly on the spectral overlap integral. Consequently, RET process requires a significant overlap between donor emission and acceptor absorption spectra. Because the emission spectra of Trp shows a good overlap with the absorption

spectra of ANS, RET between them is possible. Therefore, this donor-acceptor pair has been recently used to examine several protein-surfactant systems [42].

Fig. (6) shows the combined spectra of the Trp-ANS pair in a system with a fixed protein concentration (30  $\mu$ M), increasing ANS concentrations, and in the presence of 2 mM OTG. Spectra in Fig. (6) show that as the ANS concentration increases, the quenching of Trp occurs accompanied by successive enhancement in ANS fluorescence. In Fig. (7) we show the effect of the surfactant addition on the efficiency of the RET process as obtained by the sensitized acceptor fluorescence. Data in Fig. (7) show that at low surfactant concentration (2 mM, well below cmc) the RET process is slightly reduced. Since the RET process is strongly dependent upon the donor-acceptor distance, it may be anticipated that the presence of 2 mM OTG should produce a certain effect on the protein conformational structure, which produces a larger separation between donor and acceptor. However, when the surfactant concentration present in the system is well above the cmc (20 mM) the reduction observed in the sensitized acceptor fluorescence is much more significant. This behaviour can be due to two effects, namely: (i) a real reduction in the efficiency of the RET process as a result of the decrease in the overlap spectral due to the blue shift produced in the emission band of the donor (Trp) (see Fig. 3), which should be interpreted in the sense of a greater separation between donor and acceptor and, consequently, a certain alteration in the protein structure, and (ii) the possible displacement of some ANS molecules previously bound to the protein, caused by the surfactant binding, which should be probably transferred either to the micellar clusters adsorbed on the protein surface or even to the free micelles of surfactant. With the aim of examining this second possibility, we have studied the effect of the surfactant addition on the fluorescence of ANS. Fig. (8) shows the relative fluorescence intensity of ANS solubilized in BSA as a function of the total OTG concentration. ANS fluorescence is extremely sensitive to changes in the probe microenvironment. This probe shows in water an emission maximum at 515 nm with a emission quantum yield of 0.004, but solubilized in 1% BSA the emis-

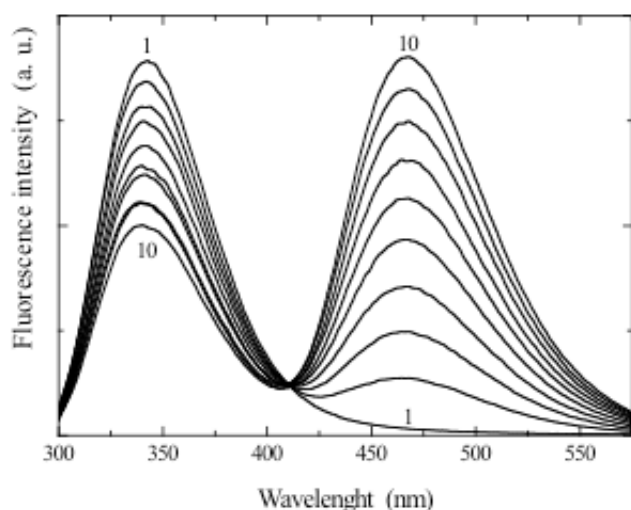


Fig. (6). Fluorescence spectra of BSA solutions (30  $\mu$ M) in 2 mM OTG and varying concentrations of ANS: 1  $\rightarrow$  0 mM and 10  $\rightarrow$  0.15 mM. ( $\lambda_{exc}$  = 295 nm).

sion maximum is blue shifted to 472 nm and its emission quantum yield is considerably enhanced ( $\approx$  0.7), a much higher value than that in micelles ( $\approx$  0.2) [42, 55]. Data in Fig. (8) show that the ANS fluorescence decreases with increasing the concentration of surfactant. These results clearly indicate that, from a certain surfactant concentration ( $>$  2 mM), some bound ANS molecules are displaced from the protein surface, being transferred to different environments where its fluorescence quantum yield is considerably reduced. Consequently, it can be concluded that, whereas data in Fig. (7) at 2 mM OTG corresponds to a real process of energy transfer, those at 20 mM OTG seem to be the result of two contributions: a energy transfer process and the displacement of a number of acceptor molecules from the protein surface to micellar-like aggregates adsorbed on the protein or to the free micelles of the surfactant. Therefore, we cannot extract definitive conclusions from the energy transfer data obtained in the presence of 20 mM OTG.

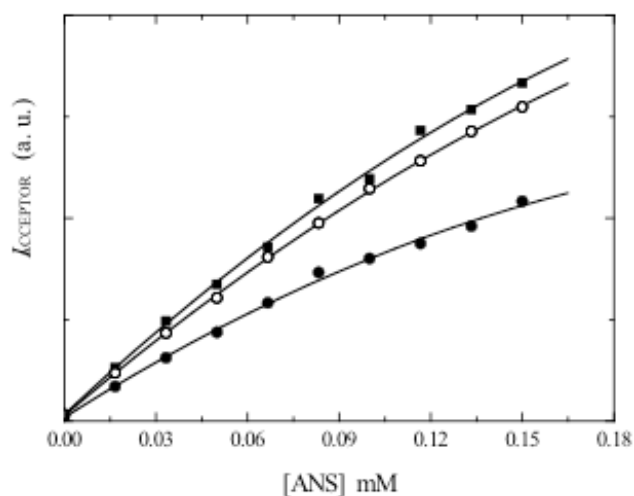


Fig. (7). Enhancement of ANS emission due to the energy transfer process in the Trp-ANS system, at a fixed protein concentration (30  $\mu$ M), as a function of its concentration at different surfactant concentrations: (■) 0 mM, (○) 2 mM, (●) 20 mM.

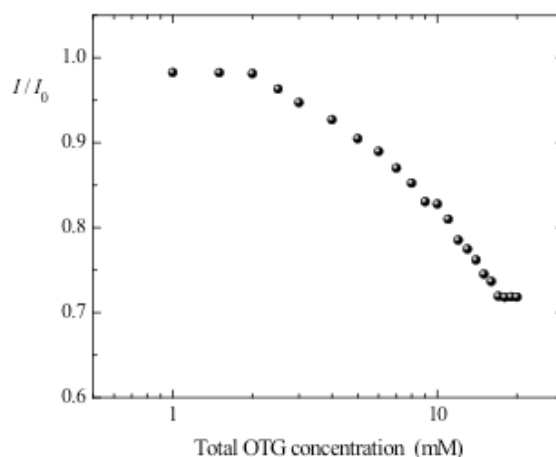
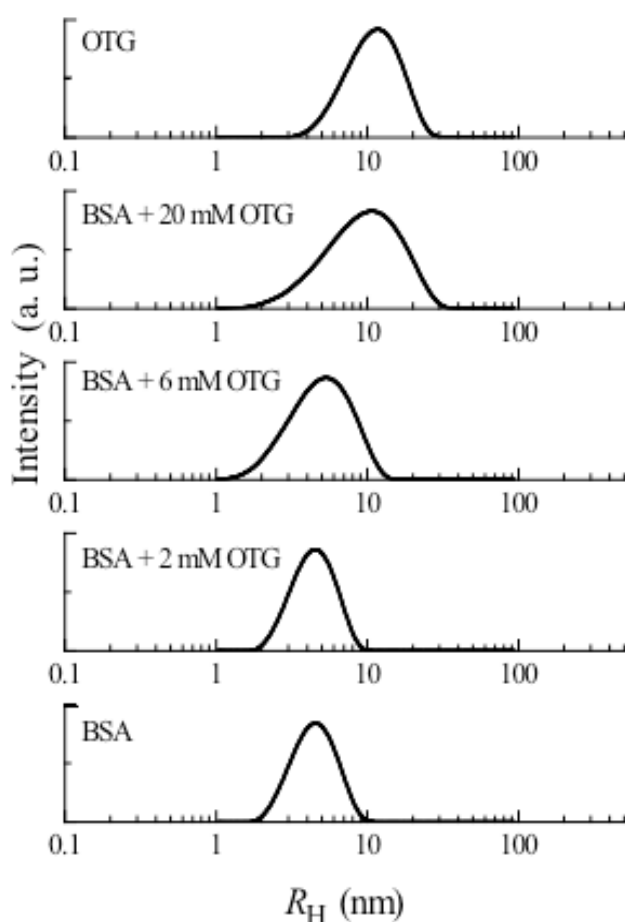


Fig. (8). Relative fluorescence intensity of ANS (20  $\mu$ M) in BSA (30  $\mu$ M) as a function of the total surfactant concentration.  $I$  and  $I_0$  are the fluorescence intensities of ANS in the presence and absence of surfactant, respectively.

## DLS Studies

With the aim of gaining additional information on the size and structures of the surfactant-protein complexes arising as a result of the binding process, we have carried out DLS measurements on surfactant-protein mixed solutions. In these experiments, solutions with a fixed protein concentration (30  $\mu\text{M}$ ) and increasing amounts of surfactants, ranging from pre- to post-micellar concentrations, were used. Fig. (9) shows the distribution of scattered intensities as a function of the apparent hydrodynamic radius,  $R_H$ , for some of the cases studied. In Fig. (9) there are a number of interesting aspects that deserve to be commented. First of all, it is to be noted that the analysis of both pure and mixed systems revealed a unimodal distribution of aggregates, which increase in size when the surfactant rises above the cmc. Second, it is observed that the free micelles of OTG and the protein alone present sizes well different (10.0 nm for OTG and 4.3 nm for BSA). With respect to the large size observed in the case of OTG micelles, it is important to mention that this value agrees well with previous values reported in the presence of 0.1 M NaCl [30, 36]. Third, the distribution patterns of the protein alone and with 2 mM OTG are rather identical, suggesting that the protein structure is practically unaffected by the surfactant binding. However, in the presence of 6 mM OTG (still below cmc) the distribution pattern is wider than



**Fig. (9).** Hydrodynamic radii distribution from dynamic light scattering measurements carried out with solutions of constant protein concentration, 30  $\mu\text{M}$ , and increasing surfactant concentrations for the BSA/OTG system.

that of BSA and where a maximum is shifted to higher values of  $R_H$ . This fact could be related to some conformational alteration in the protein structure due to the cooperative binding of the surfactant onto the protein. Finally, when the surfactant concentration is well above the cmc (20 mM), it is observed that the peak of the distribution corresponds with that of the free OTG micelles formed at the same surfactant concentration, but its bandwidth is greater. A possible explanation for this fact is that the intensity distribution of the mixed system in the presence of 20 mM OTG is the result of the superposition of two dispersant species: the protein-surfactant complexes and the free micelles of the surfactant. In order to check this possibility, we have made an attempt of discriminating between the two scattering species by using a treatment based on the analysis of the autocorrelation functions according to the strategy described below.

In a DLS experiment, the digital correlator measures the intensity autocorrelation function  $g_I(t)$ , which is related to the field autocorrelation function  $g_E(t)$  for a Gaussian scattering process through Siegert relation [56]

$$g_I = 1 + C |g_E(t)|^2 \quad (10)$$

where  $t$  is the delay time and  $C$  is the Siegert constant, an experimental fitting parameter of the measuring device. For a dilute dispersion of non-interacting macromolecules,  $g_E(t)$  decays exponentially according to

$$g_E(t) = \exp\left(-\frac{t}{\tau}\right) \quad (11)$$

where  $\tau$  is the relaxation time, which is related to the so-called apparent diffusion coefficient,  $D$ , by

$$\tau = \frac{1}{Dq^2} \quad (12)$$

here  $q$  is the scattering vector, which is related to the dispersion angle,  $\alpha$ , by  $q = (4\pi n_0/\lambda)\sin(\alpha/2)$ , with  $n_0$  the refractive index of the solvent and  $\lambda$  the wavelength of light in vacuum.

In the case of a sample with  $N$  different scattering species, with relaxation times  $\tau_i$  and diffusion coefficients  $D_i$ , the autocorrelation functions of the field and intensity are given, respectively, by

$$g_E = \sum_{i=1}^N a_i \exp\left(-\frac{t}{\tau_i}\right) \quad (13)$$

and

$$g_I(t) = A + \left[ \sum_{i=1}^N a_i \exp\left(-\frac{t}{\tau_i}\right) \right]^2 \quad (14)$$

In the case of two different sizes of scattering species, the equation (14) can be expressed as

$$g_I(t) = A + \left[ a_1 \exp\left(-\frac{t}{\tau_1}\right) + a_2 \exp\left(-\frac{t}{\tau_2}\right) \right]^2 \quad (15)$$

where  $a_1$  and  $a_2$  are expansion coefficients known as amplitudes, which represent the relative contributions of each particle size, and  $\tau_1$  and  $\tau_2$  are the relaxation times of the respective species. It has been established that these relaxation times must differ by at least a factor of two in order to obtain statistically significant regression [54]. Equation (12) allows for the determination of the diffusion coefficients and then the hydrodynamic radii can be obtained by

$$R_H = \frac{k_B T}{6\pi\eta_0 D} \quad (16)$$

where  $\eta_0$  is the solvent viscosity,  $k_B$  is the Boltzmann constant and  $T$  is the absolute temperature of the dispersion.

Following to Hitscherich *et al.* [57], the appropriate number of exponentials required to fit an autocorrelation function was determined by the relative weight of the two exponential terms of equation (15). The criterion employed was the following: as long as  $a_2 \leq 0.1 a_1$  we use a single exponential fit, but when  $a_2 > 0.1 a_1$  the autocorrelation functions were fitted to a double exponential. The obtained parameters are listed in Table 2, where we also present the hydrodynamic radius and the polydispersity index as determined by considering an only population of scattering species. From data in Table 2, it is firstly seen that below the cmc of the surfactant ( $\leq 10$  mM) only single scattering species with relaxation times ranging between 27 and 30  $\mu$ s are observed. But when the surfactant concentration is well above the cmc two relaxation times appear. In the pre-micellar region, it is observed that the relaxation time slightly increase with the surfactant concentration. This increase is, of course, reflected in the behaviour of the corresponding hydrodynamic radius  $R_1$ , which increases from a value of 4.6 nm for the protein alone to 5.3 nm for the surfactant-protein complex. This growth (around 15 %) suggests a partial protein denaturation induced by the surfactant binding, in accordance with our previous findings; particu-

larly, those involving changes in the emission spectrum of the intrinsic fluorescence of BSA (see Fig. 3). Above 8 mM OTG the value of  $R_1$  remains rather constant. However, above 10 mM arises a second species whose relaxation time (and hydrodynamic radius) seems to correspond with that of the OTG free micelles. When the saturation takes place, which happens near the cmc, it is observed that two types of structures coexist in the medium; surfactant-protein complexes and free micelles of the surfactant. On the other hand, the values of  $R_H$  as obtained by the mono-exponential analysis compare well with the  $R_1$  values in the pre-micellar region. However, the apparent increase in  $R_H$  observed in the post-micellar region actually reflects the superposition of the two coexisting species. Whereas the size of the surfactant-protein complexes remains constant, that of the surfactant free micelles increases with the surfactant concentration. In this context, the tendency of PDI (see Table 2) is also significant. Note that, in the pre-micellar region, PDI increases with the surfactant concentration, as expected. Nevertheless, from 10 mM OTG, the PDI value decreases until reaching a value close 0.1. This reduction reflects the fact that the higher molecular-weight component (that is, the free micelles) is predominant in the medium and, hence, controls the polydispersity index.

According to our observations, a model analogous to that schematically represented in Fig. (10) mimicking the interactions between OTG and BSA can be proposed. Two different experimental situations must be considered. At low surfactant concentration, that is, as long as the free surfactant concentration is below the cmc, the surfactant binds to BSA through a non-cooperative mechanism mainly controlled by hydrophobic interactions. The hydrophobic chains of OTG would be adsorbed on the protein surface with their head groups directed toward the bulk water and the protein acting as a nucleus on which OTG monomers condense below the cmc. In this concentration range the binding process would probably lead to some minor conformational change in the protein structure and, as a result, to a slight increase in the

**Table 2.** Relaxation times ( $\tau_i$ ), diffusion coefficients ( $D_i$ ) and hydrodynamic radii ( $R_i$ ) obtained from the fit of the autocorrelations functions according to the equation (14) by using either a single or a double exponential fitting (see text), together with the values of the hydrodynamic radii ( $R_H$ ) and the polydispersity indexes (PDI) as determined by considering an only population of scattering species

[OTG] (mM)	$\tau_1$ ( $\mu$ s)	$\tau_2$ ( $\mu$ s)	$D_1 \times 10^{11}$ ( $m^2/s$ )	$D_2 \times 10^{11}$ ( $m^2/s$ )	$R_1$ (nm)	$R_2$ (nm)	$R_H$ (nm)	PDI
0	26.96		5.32		4.6		4.3	0.205
2	28.40		5.05		4.9		4.5	0.254
4	28.54		5.03		4.9		4.5	0.249
6	28.62		5.01		4.9		4.5	0.232
8	30.68		4.68		5.2		4.7	0.269
10	31.26		4.59		5.3		4.9	0.310
15	29.96	70.30	4.79	2.04	5.1	12.0	6.1	0.214
20	30.32	62.72	4.73	2.29	5.2	10.7	8.1	0.184
OTG		60.58		2.37		10.4	10.0	0.103

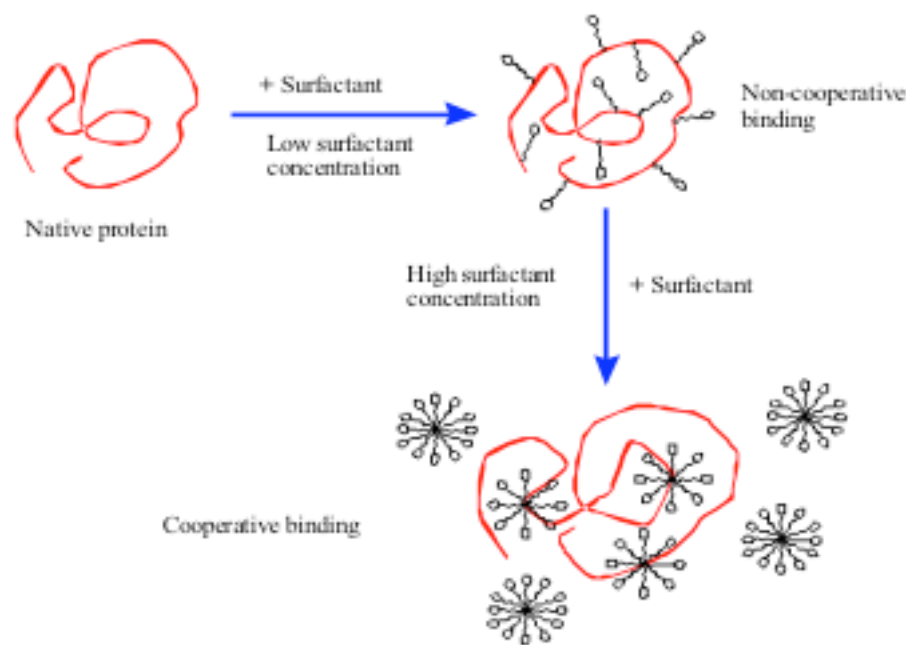


**Fig. (10).** A schematic representation of the proposed binding model for the interaction between OTG and BSA. At low surfactant concentration, below cmc, monomers of surfactant are adsorbed on the protein by a non-cooperative mechanism. In the presence of an excess of surfactant, above cmc, a cooperative mechanism operates, producing surfactant-protein complexes coexisting with the free micelles of the surfactant.

size of the complex, but where no free micelles would be present. However, when the surfactant concentration becomes high enough, a cooperative mechanism operates, leading to the formation of micelle-like structures adsorbed onto the protein surface and to the formation of free micelles of the surfactant. At this stage, a partial protein denaturation should be expected, and saturated protein-surfactant complexes and free micelles will coexist in the system.

## CONCLUSIONS

An experimental study on the interaction between OTG and the globular protein BSA has been carried out. From the obtained results we can extract the following conclusions:

1. The binding of OTG to BSA has been demonstrated by both the pyrene 1:3 ratio index measurements and the surface tension data in the air-liquid interface.
2. Quenching of the BSA fluorescence together with a marked decrease in its emission maximum at high surfactant concentration suggest a partial denaturation of the protein as a result of the surfactant binding.
3. The procedure based on the surface tension measurements seems to underestimate the average number of bound surfactant monomers per protein molecule, particularly to high protein concentration. However, our binding studies at low protein concentration suggest a binding non-cooperative mechanism, which becomes cooperative when the surfactant concentration is high enough.
4. The formation of clusters of surfactant adsorbed onto the protein surface was confirmed by the determination of the average aggregation numbers in the absence and in the presence of protein. From these results, a conceptual

scheme based on the so-called “necklace and bead” model has been proposed.

5. The RET studies at low surfactant concentration revealed a slight conformational change in the protein structure. However, at high surfactant concentration our results were inconclusive, because of the displacement of the acceptor molecules from the protein surface as a consequence of the surfactant binding.
6. By applying appropriate fitting techniques to the auto-correlation functions, it was possible to discriminate between two scattering species: surfactant-protein complexes and free micelles of the surfactant, coexisting in equilibrium in the OTG/BSA system.

## ACKNOWLEDGMENTS

This work has been financially supported by the Spanish Education and Science Ministry (Project CTQ2005-04513).

## REFERENCES

- [1] Israelachvili, J. N.; Marcelja, S.; Horn, R. G. Physical principles of membrane organization. *Q. Rev. Biophys.*, **1980**, *13*(2), 121-200.
- [2] Tanford, C. *The hydrophobic effect: formation of micelles and biological membranes*. Wiley-Interscience, New York, **1980**.
- [3] le Marie, M.; Champeil, P.; Møller, J. V. Interaction of membrane proteins and lipids with solubilizing detergents. *Biochim. Biophys. Acta*, **2000**, *1508*(1-2), 86-111.
- [4] Garavito, R.M.; Ferguson-Miller, S. Detergents as tools in membrane biochemistry. *J. Biol. Chem.*, **2001**, *276*(35), 32403-32406.
- [5] Jones, M. N. Surfactant interactions with biomembranes and proteins. *Chem. Soc. Rev.*, **1992**, *21*(2), 127-136.
- [6] Ananthapadmanabhan, K.P. In: *Interactions of surfactants with polymers and proteins*. Goddard, E. D., Ananthapadmanabhan, K.P., Eds.; CRC Press Inc., London, **1993**; pp. 319-365.
- [7] Peters, T. Jr. *All about albumin biochemistry, genetics, and medical applications*. Academic Press. San Diego, C.A. **1996**.

- [8] Schweitzer, B.; Felipe, A. C.; Dal Bó, A.; Minatti, E.; Zanette, D. Competitive process of binding between the anionic surfactants sodium dodecyl sulfate and sodium cholate in bovine serum albumin. *Macromol. Symp.*, **2005**, 229(1), 208-216.
- [9] Santos, S. F.; Zanette, D.; Fischer, H.; Itri, R. A systematic study of bovine serum albumin (BSA) and sodium dodecyl sulfate (SDS) interactions by surface tension and small angle X-ray scattering. *J. Colloid Interface Sci.*, **2003**, 262(2), 400-408.
- [10] Turro, N.J.; Lei, X.-G.; Ananthapadmanabhan, K.P.; Aronson, M. Spectroscopic probe analysis of protein-surfactant interactions - the BSA/SDS system. *Langmuir*, **1995**, 11(7), 2525-2533.
- [11] Gelamo, E. L.; Tabak, M. Spectroscopic studies in the interaction of bovine (BSA) and human (HSA) serum albumins with ionic surfactants. *Spectrochim. Acta Part A*, **2000**, 56(11), 2255-2271.
- [12] Gelamo, E. L.; Silva C.J.T.P.; Imasato, H.; Tabak, M. Interaction of bovine (BSA) and human (HSA) serum albumins with ionic surfactants: spectroscopy and modelling. *Biochim. Biophys. Acta*, **2002**, 1594(1), 84-99.
- [13] Das, R.; Guha, D.; Mitra, S.; Kar, S.; Lahiri, S.; Mukherjee, S. Intramolecular charge transfer as probing reaction: fluorescence monitoring of protein-surfactant interactions. *J. Phys. Chem. A*, **1997**, 101(22), 4042-4047.
- [14] Guo, X.-H.; Chen, S.-H. The structure and thermodynamics of protein-SDS complexes in solution and the mechanism of transports in gel electrophoresis process. *Chem. Phys.*, **1990**, 149(1-2), 129-139.
- [15] Valstar, A.; Vasilescu, M.; Vigouroux, C.; Stilbs, P.; Almgren, M. Heat-set bovine serum albumin-sodium dodecyl sulfate gels studied by fluorescence probe methods, NMR, and light scattering. *Langmuir*, **2001**, 17(11), 3208-3215.
- [16] Stenstam, A.; Khan, A.; Wennerström, H. The lysozyme-dodecyl sulfate system. An example of protein-surfactant aggregation. *Langmuir*, **2001**, 17(24), 7513-7520.
- [17] Deo, N.; Jockusch, S.; Turro, N.J.; Somasundaram, P. Surfactant interactions with zein protein. *Langmuir*, **2003**, 19(12), 5083-5088.
- [18] Sabín, J.; Prieto, G.; González-Pérez, A.; Ruso, J. M.; Sarmiento, F. Effects of fluorinated surfactants on human serum albumin at different pHs. *Biomacromolecules*, **2006**, 7(1), 176-182.
- [19] Cserháti, T. Alkyl ethoxylated and alkylphenol ethoxylated non-ionic surfactants: interaction with bioactive compounds and biological effects. *Environ. Health Perspect.*, **1995**, 103(4), 358-364.
- [20] Singh K. S.; Kishore, N. Thermodynamic insights into the binding of triton X-100 to globular proteins: a calorimetric and spectroscopic investigation. *J. Phys. Chem. B*, **2006**, 110(19), 9728-9737.
- [21] Saito, S.; Tsuchiya, T. Characteristics of *n*-octyl- $\beta$ -D-thiogluco-pyranoside, a new non-ionic detergent useful for membrane biochemistry. *Biochem. J.*, **1984**, 222(3), 829-832.
- [22] Wenk, M. R.; Seelig, J. Interaction of octyl- $\beta$ -thiogluco-pyranoside with lipid membranes. *Biophys. J.*, **1997**, 73(5), 2565-2574.
- [23] del Burgo, P.; Junquera, E.; Aicart, E. Mixed micellization of a nonionic-cationic surfactant system constituted by *n*-octyl- $\beta$ -D-thiogluco-pyranoside/dodecyltrimethylammonium bromide/H<sub>2</sub>O. An electrochemical, thermodynamic, and spectroscopic study. *Langmuir*, **2004**, 20(5), 1587-1596.
- [24] Molina-Bolívar, J. A.; Aguiar, J.; Peula-García, J. M.; Carnero Ruiz, C. Surface activity, micelle formation, and growth of *n*-octyl- $\beta$ -D-thiogluco-pyranoside in aqueous solutions at different temperatures. *J. Phys. Chem. B*, **2004**, 108(34), 12813-12820.
- [25] Antonelli, M. L.; Bonicelli, M. G.; Ceccaroni, G.; La Mesa, C.; Sesta, B. Solution properties of octyl- $\beta$ -D-glucoside. 2. Thermodynamics of micelle formation. *Colloid Polymer Sci.*, **1994**, 272(6), 704-711.
- [26] Chami, M.; Pehau-Arnaudet, G.; Lambert, O.; Rank, J.-L.; Lévý, D.; Rigaud, J.-L. Use of octyl- $\beta$ -thiogluco-pyranoside in two dimensional crystallization of membrane proteins. *J. Struct. Biol.*, **2001**, 133(1), 64-74.
- [27] Brackman, J. C.; van Os, N. M.; Engberts, J.B.F.N. Polymer-nonionic micelle complexation. Formation of poly(propylene oxide)-complexed *n*-octyl thiogluco-side micelles. *Langmuir*, **1988**, 4(6), 1266-1269.
- [28] Winnik, F. M. Interaction of fluorescent dye labeled (hydroxypropyl)cellulose with nonionic surfactants. *Langmuir*, **1990**, 6(2), 522-524.
- [29] Winnik, F. M.; Ringsdorf, H.; Venzmer, J. Interactions of surfactants with hydrophobically modified poly(*N*-isopropylacrylamides). 1. Fluorescence probe studies. *Langmuir*, **1991**, 7(5), 905-911.
- [30] Diab, C.; Winnik, F. M.; Tribet, C. Enthalpy of interaction and binding isotherms of non-ionic surfactants onto micellar amphiphilic polymers (amphipols). *Langmuir*, **2007**, 23(6), 3025-3035.
- [31] Kalyanasundaram, K.; Thomas, J.K. Environmental effects on vibronic band intensities in pyrene monomer fluorescence and their application in studies of micellar systems. *J. Am. Chem. Soc.*, **1977**, 99(7), 2039-2044.
- [32] Turro, N.J.; Yekta, A. Luminescent probes for detergent solutions. A simple procedure for determination of the mean aggregation number of micelles. *J. Am. Chem. Soc.*, **1978**, 100(18), 5951-5952.
- [33] Vasilescu, M.; Angelescu, D.; Almgren, M.; Valstar, A. Interactions of globular proteins with surfactants studied with fluorescence probe methods. *Langmuir*, **1999**, 15(8), 2635-2643.
- [34] Carnero Ruiz, C.; Hierrezuelo, J. M.; Aguiar, J.; Peula-García, J. M. Physicochemical Studies on the Interaction between *N*-Decanoyl-*N*-methylglucamide and Bovine Serum Albumin. *Biomacromolecules*, **2007**, 8(8), 2497-2503.
- [35] Aguiar, J.; Carpena, P.; Molina-Bolívar, J.A.; Carnero Ruiz, C. On the determination of the critical micelle concentration by the pyrene 1:3 ratio method. *J. Colloid Interface Sci.*, **2003**, 258(1), 116-122.
- [36] Molina-Bolívar, J. M.; Hierrezuelo, J. M.; Carnero Ruiz, C. Effect of NaCl on the self-aggregation of *n*-octyl  $\beta$ -D-thiogluco-pyranoside in aqueous medium. *J. Phys. Chem. B*, **2006**, 110(24), 12089-12095.
- [37] Nishikido, N.; Takahara, T.; Kobayashi, H.; Tanaka, M. Interaction between hydrophilic proteins and nonionic detergents studied by surface tension measurements. *Bull. Chem. Soc., Jpn.*, **1982**, 55(10), 3085-3088.
- [38] Tribout, M.; Paredes, S.; González-Mañas, J.M.; Goñi, F.M. Binding of triton X-100 to bovine serum albumin as studied by surface tension measurements. *J. Biochem. Biophys. Methods*, **1991**, 22(2), 129-133.
- [39] Nishiyama, H.; Maeda, H. Reduced lysozyme in solution and its interaction with non-ionic surfactants. *Biophys. Chem.*, **1992**, 44(3), 199-208.
- [40] Zadymova, N.M.; Yampol'skaya, G.P.; Filatova, L.Y. Interaction of bovine serum albumin with nonionic surfactant tween 80 in aqueous solutions: complexation and association. *Colloid J.*, **2006**, 68(2), 162-172.
- [41] Andreu, J. M.; Muñoz, J. M. Interaction of tubulin with octyl glucoside and deoxycholate. 1. Binding and hydrodynamic studies. *Biochemistry*, **1986**, 25(18), 5220-5230.
- [42] De, S.; Girigoswami, A.; Das, S. Fluorescence probing of albumin-surfactant interaction. *J. Colloid Interface Sci.*, **2005**, 285(2), 562-573.
- [43] De, S.; Das, S.; Girigoswami, A. Spectroscopy probing of bile salt-albumin interaction. *Colloids Surf. B*, **2007**, 54(1), 74-81.
- [44] Pi, Y.; Shang, Y.; Peng, C.; Liu, H.; Hu, Y.; Jiang, J. Interactions between bovine serum albumin and gemini surfactants alkanedyl- $\alpha$ ,  $\omega$ -bis(dimethyldodecylammonium bromide). *Biopolymers*, **2006**, 83(3), 243-249.
- [45] Jones, M. N. A theoretical approach to the binding of amphipathic molecules to globular proteins. *Biochem. J.*, **1975**, 151(1), 109-114.
- [46] Córdoba, J.; Reboiras, M. D.; Jones, M. J. Interaction of *n*-octyl- $\beta$ -D-thiogluco-pyranoside with globular proteins in aqueous solution. *Int. J. Biol. Macromol.*, **1988**, 10(5), 270-276.
- [47] Sukow, W. W.; Sandberg, H. E.; Lewis, E. A.; Eatough, D. J.; Hansen, L. D. Binding of the triton X series of nonionic surfactants to bovine serum albumin. *Biochemistry*, **1980**, 19(5), 912-917.
- [48] Nielsen, A. D.; Borch, K.; Westh, P. Thermochemistry of the specific binding of C12 surfactants to bovine serum albumin. *Biochim. Biophys. Acta*, **2000**, 1479(1-2), 321-331.
- [49] Balzer, D. Cloud point phenomena in the phase-behavior of alkyl polyglucosides in water. *Langmuir*, **1993**, 9(12), 3375-3384.
- [50] Zana, R. In *Surfactants solutions: new methods of investigation*, R. Zana (Ed.), Marcel Dekker, New York, **1987**, pp. 241-294.
- [51] Lindman, B.; Thalberg, K. In: *Interactions of surfactants with polymers and proteins*. Goddard, E.D.; Ananthapadmanabhan, K.P. Eds. CRC press. London, **1993**, pp. 203-276.
- [52] Wu, P. G.; Brand, L. Resonance energy transfer: methods and applications. *Anal. Biochem.*, **1994**, 218(1), 1-13.
- [53] Hayakawa, K.; Nakano, T.; Satake, I.; Kwak, J.C.T. Energy transfer between pyrene and proflavine solubilized in polymer/surfactant complexes. *Langmuir*, **1996**, 12(2), 269-275.

- [54] Förster, T. Experimentelle und theoretische untersuchung des zwischenmolekularen ubergangs von elektronenanregungsenergie. *Z. Naturforsch.*, **1949**, 4A, 321-327.
- [55] Slavik, J. Anilinoaphthalene sulfonate as a probe of membrane composition and function. *Biochim. Biophys. Acta*, **1982**, 694(1), 1-25.
- [56] Berne, B.J.; Pecora, R. *Dynamic Light Scattering. With applications to Chemistry, Biology, and Physics*, Dover Publications. New York, **2000**.
- [57] Hitscherich, C.; Aseyev, V.; Wiencek, J.; Loll, P. J. Effects of PEG on detergent micelles: implications for the crystallization of integral membrane proteins. *Acta. Cryst.*, **2001**, D57, 1020-1029.

---

Received: April 22, 2008

Revised: May 05, 2008

Accepted: May 06, 2008

© Ruiz et al.; Licensee Bentham Open.

This is an open access article distributed under the terms of the Creative Commons Attribution License (<http://creativecommons.org/licenses/by/2.5/>), which permits unrestricted use, distribution, and reproduction in any medium, provided the original work is properly cited.